phys. stat. sol. (b) **221**, 43 (2000)

Subject classification: 71.35.Cc; 71.45.Gm; 78.55.Cr; 78.66.Fd; S7.12

Carrier–Carrier Correlations and Their Effect on Optically Excited Single Semiconductor Quantum Dots

E. DEKEL (a), D. REGELMAN (a), D. GERSHONI (a), E. EHRENFREUND (a), W. V. SCHOENFELD (b), and P. M. PETROFF (b)

(a) Physics Department and Solid State Institute, Technion–Israel Institute of Technology, Haifa 32000, Israel

(b) Materials Department, University of California, Santa Barbara, CA 93106, USA

(Received April 10, 2000)

We resolve spatially, spectroscopically and temporally the photoluminescence emission from single self-assembled In(Ga)As/GaAs quantum dots. The rich photoluminescence spectrum and its evolution with time after pulse excitation and with the density of excitation is experimentally measured and analyzed using a theoretical multiexciton model. From the quantitative agreement between the measured and calculated spectra, the radiative lifetime of a single quantum dot exciton is unambiguously determined.

Optical studies of semiconductor quantum dots in general and self-assembled quantum dots (SAQDs) in particular [1 to 6] have been a subject of very intensive investigations for quite some time. These reports brought strong spectral evidences that the presence of few confined carriers in such a small volume gives rise to correlated few carrier multiplexes, which are unstable otherwise. Specifically, we have established [5,6]. that confined carriers exchange terms are most instrumental for the understanding of the experimental results when more than two carriers of the same type participate in the radiative process [5 to 7].

In this study we present continuous wave (cw) and time resolved spectroscopical studies of the dynamics and recombination processes of photogenerated carriers confined in single In(Ga)As/GaAs SAQDs. The hosting layers of these dots, unlike those of our previous studies [5,6] contain no aluminum. Therefore, the nonradiative decay rates are greatly reduced [8], and their significantly enhanced PL emission makes it easier to facilitate time correlated single photon counting techniques [9 to 11].

The theoretical model which we have previously developed [6] is extended here to quantitatively analyze our low light level time resolved photoluminescence (PL) measurements. Our model systematically explains the measured cw and time resolved PL spectra and it quantitatively accounts for the dependence of the PL spectra on time and excitation density. In particular, it describes well the dynamics of the photoexcited carriers and determines the radiative decay rates of the correlated excitons (multiexcitons).

The SAQD sample was grown by molecular beam epitaxy of a strained epitaxial layer of InAs on (100) oriented GaAs substrate. Small islands of In(Ga)As connected by a very thin wetting layer are thus formed in the Stranski-Krastanov [12] growth mode. The vertical and lateral dimensions of the InAs SAQDs were adjusted during

growth by the partially covered island growth technique [13]. The uncapped dots were found to have base dimensions of 45 nm by 40 nm and height of 4.5 nm by the use of atomic force microscopy. The sample was not rotated during the growth of the SAQD layer, therefore a gradient in the QDs density was formed and low density areas, in which the average distance between neighboring QDs is larger than our optical spatial resolution, could easily be found on the sample surface. We use a diffraction limited low temperature confocal optical microscope for the photoluminescence (PL) studies of the single SAQDs. The setup is described in detail elsewhere [6].

For time resolved spectroscopy the dispersed light from the 0.22 m monochromator was focused onto a small, thermo-electrically cooled, single channel avalanche silicon photodiode. The signal from the photodiode was analyzed using conventional photon counting electronics.

We locate an optically excited SAQD by scanning the sample surface while monitoring the resulted PL spectra. Once a typical emission spectrum from a SAQD is observed the scan is terminated and the objective position is optimized above the dot.

In Fig. 1a we display typical PL spectra from a single SAQD for various cw excitation powers at photon energy of 2.25 eV. At the lowest excitation density (0.01 μW), a single narrow spectral line is observed at energy of 1.284 eV. We denote this line by A_1. Its linewidth at this excitation density is limited by the spectral resolution of our system (0.2 meV). As the excitation density increases, two notable changes in the PL spectrum occur: First, a satellite spectral line, A_2, appears 3.5 meV below A_1. Second, a higher energy spectral line, B_1, emerges at 1.324 eV, 40 meV above the first line to be observed, A_1. At yet higher excitation power, an additional spectral line, B_2, develops

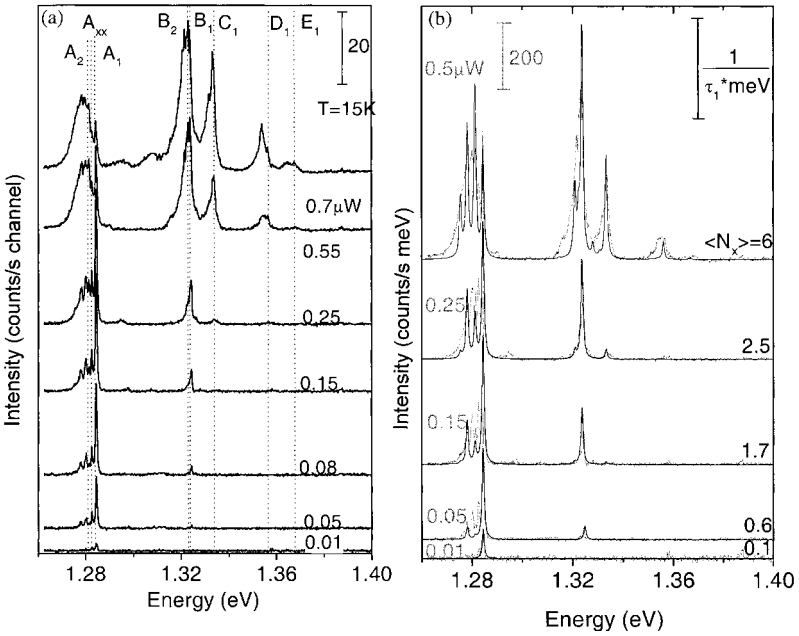

Fig. 1. a) Measured and b) calculated single SAQD PL spectra at various cw excitation powers. The spectra are vertically shifted for clarity. $\langle N_x \rangle$ is the average number of excitons

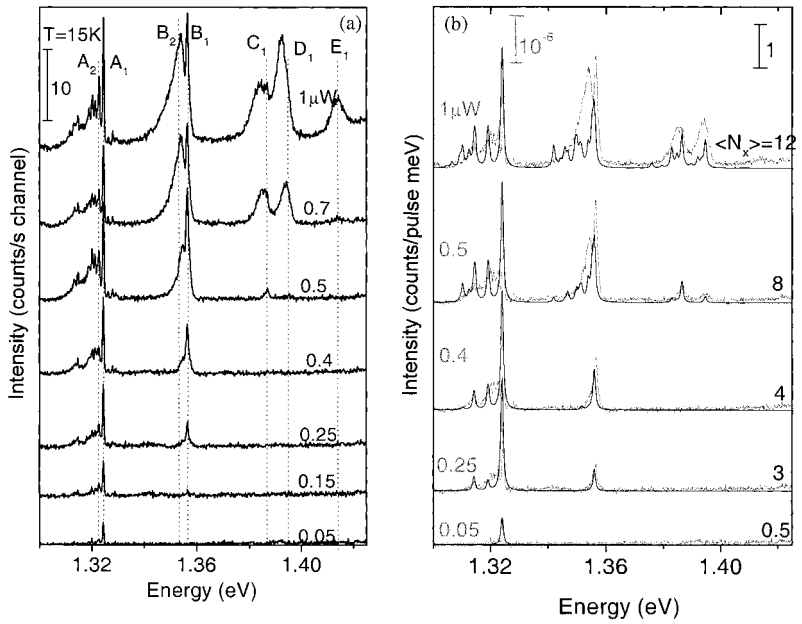

Fig. 2. a) Measured and b) calculated single SAQD PL spectra at various pulse excitation powers. The curves are vertically shifted for clarity. $\langle N_x \rangle$ is the average number of excitons

1.5 meV lower in energy than B_1. Further increase in the excitation power results in an increase in the number of satellites, gradually forming spectral emission bands to the lower energy side of the lines A_1 and B_1, respectively. In addition, new higher energy groups of spectral lines, C, D and E, respectively, gradually emerge and similarly develop their own satellites and lower energy spectral bands. For clarity, we mark the various spectral lines by letters and numerical subscripts, representing, respectively, the energy group to which the spectral lines belong and their appearance order with increasing excitation density. With the increase in power, all the observed lines at their appearance order, undergo a cycle in which their emission intensity first increases, then reaches maximum and saturates, and eventually, at yet higher excitation power, the emission intensity significantly weakens. Consequently, the various groups seem to be "red shifted" with the increase in excitation power. Our model simulations (see below), presented for comparison in Fig. 1b, duplicate this behavior.

In Fig. 2a we present PL spectra from a single SAQD for various excitation powers by picosecond short 1.750 eV laser pulses. The spectra as measured in this case represent temporal average on the PL emission. Their evolution with increasing the excitation power is similar to that observed in the cw excitation mode (Fig. 1a), except for one significant difference: With the increase in excitation power, after reaching saturation, the intensity of the emission from the various spectral lines remains constant and it does not decrease with further increase in the excitation power. Our model simulations (see below) for this case are presented for comparison in Fig. 2b.

In Fig. 3a we present the PL intensity as a function of time after the excitation pulse at a given power, for various spectral lines from Fig 2a. In general, for each spectral line there are two distinct time domains. In the first one, the emission intensity rises

with the time after the excitation and in the second it decays. For a given excitation power, the various spectral lines have different temporal responses. As a rule it is easily observed that the lower is the energy of a given spectral group of lines, the longer are their rise and decay times. Within a given group of lines, however, lower energy lines rise and decay faster. Our model calculations (see below) are presented for comparison in Fig. 3b. In Fig. 3c we display by symbols the measured rise time of the spectral lines A_1 and B_1 as a function of the excitation power. The lines in Fig. 3d represent our model calculations.

The complex task of calculating the emission spectrum which results from the radiative annihilation of a multicarrier state can be quite well approximated provided that the energy levels of single carriers within the dots are known and that, in addition, the exchange integrals between these levels are known as well [6]. In order to calculate these values, an exact knowledge of the quantum dot dimensions, geometrical shape, composition and strain field has to be given [14 to 16]. At this stage, it is unrealistic to expect such a detailed knowledge for each SAQD. Fortunately, these energies can be, to a large extent, deduced directly from the measured QD emission spectrum. For ex-

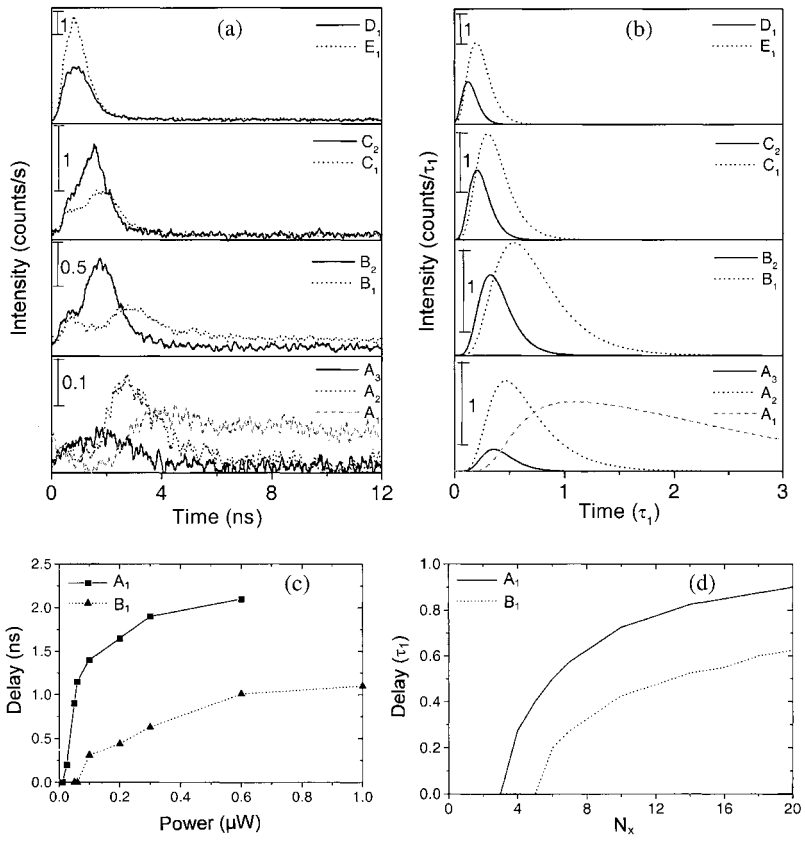

Fig. 3. a) Measured and b) calculated PL emission intensity as a function of pulse excitation power for various spectral lines from Fig. 2. c) Measured and d) calculated delay times of the spectral lines A_1 and B_1

ample, it is quite obvious that the single line that we observe at low excitation density (line A_1) is due to the recombination of a single exciton within the optically excited SAQD. Similarly, it follows that the first line in the higher energy group of spectral lines (line B_1) is due to the recombination of an electron–hole pair in their respective second energy levels. Lines C_1 and D_1 similarly mark higher energy optical transitions due to the recombination of electron–hole pairs at their respective third and fourth single carrier energy levels, respectively. As we demonstrated in Ref. [5] the combined electron–electron and hole–hole exchange energy between their first and second single carrier levels is given precisely by the energy difference between line A_1 and line A_2. Similarly, the energy difference between the spectral lines B_1 and B_2 is an exact measure for the combined exchange energy between the first and third single carrier energy states.

The e–e and h–h exchange-interactions are responsible for the line splitting described in Figs. 1a and 2a. In addition, they give rise to a spectral red shift of optical transitions from successively higher order multiexcitons, as we demonstrated previously [5]. This red shift is caused by the number of exchange interactions, which increases with the number of carriers. Therefore, the sum of exchange interaction energies lowers the energy of the $N_x + 1$ multiexciton levels more than it lowers the energy of the N_x multiexciton levels, thus causing successive red shift in the transition energies.

In order to understand the spectral evolution of the SAQD PL with excitation density and with time after pulse excitation a knowledge of the various recombination rates of a particular multiexcitonic state is required. Exact calculation of these rates, requires exact knowledge of the confined single carriers wave functions, which is unrealistic to expect. We estimate these rates using the following simplifications: Only optical transitions in which a photon is emitted as a result of the annihilation of one electron–hole pair is considered. We use the dipole approximation for calculating the optical transition rate between initial and final multiexcitonic states and we assume that the dipole matrix element for optically allowed transitions between single carrier states is equal to that of the single exciton [5,6]. Finally, only optical transitions between multiexcitonic states of same total spin and same spin projection along the growth axis are considered [5,7]. The optical recombination rates are then easily estimated by counting the number of angular momentum and symmetry conserving transitions between the initial to the final states. We assume that a multiexciton reaches thermal equilibrium and relaxes to its ground level much faster than its recombination rate. Therefore, only optical transitions from the ground energy level of each $(N_x + 1)$-th multiexciton to all possible levels of the N_x-th multiexciton are considered. Using the calculated radiative recombination rates we solve a coupled set of rate equations for the various multiexcitons within the QD. These equations are analytically solved for the cw as well as for the pulse excitation. The solutions yield the various probabilities of finding multiexcitons within the photoexcited QD [6]. Finally, we use the calculated multiexciton energies (spectrally broadened by a Gaussian of 0.5 meV width), their probabilities and the optical transition rates between them for simulating the PL emission spectra presented in Figs. 1b and 2b.

The calculated temporal evolution of the PL spectra is described in Figs. 3b and 3d. It is worth noting that the multiexciton model explains the rise time of the various spectral lines and its dependence on the excitation density. From the comparison between the measured and calculated rise time as a function of the excitation the QD

single exciton lifetime can be straightforwardly deduced. The lifetime that we obtain amounts to (2 to 4) ns. The same lifetime is independently obtained from the comparisons between the calculated and measured cw and pulsed temporally integrated spectra of Fig. 1 and 2, respectively. This lifetime, is an order (two orders) of magnitude longer than the intrinsic radiative lifetime of single excitons confined in semiconductor quantum wires [17 to 19] (quantum wells [20,21]) of comparable confining dimensions. This is due to the reduced spatial coherence between the QD confined exciton dipole moment and the extended electromagnetic radiation field.

Acknowledgements The research was supported by the US–Israel Binational Science Foundation (453/97) and the Israel Science Foundation founded by the Israel Academy of Sciences and Humanities.

References

[1] M. BAYER, T. GUTBROD, A. FORCHEL, V.D. KULAKOVSKII, A. GORBUNOV, M. MICHEL, R. STEFFEN, and K.H. WANG, Phys. Rev. B **58**, 4740 (1998).
[2] A. ZRENNER, M. MARKMANN, A.L. EFROS, M. BICHLER, W. WEGSHEIDER, G. BOHM, and G. ABSTREITER, Physica **256/258B**, 356 (1998).
[3] L. LANDIN, M.-E. PISTOL, C. PRYOR, M. PERSSON, L. SAMUELSON, and M. MILLER, Phys. Rev. B **60**, 16640 (1999).
[4] Y. TODA, O. MORIWAKI, M. NISHIOKA, and Y. ARAKAWA, Phys. Rev. Lett. **82**, 4114 (1999).
[5] E. DEKEL, D. GERSHONI, E EHRENFREUND, D. SPEKTOR, J.M. GARCIA, and P.M. PETROFF, Phys. Rev. Lett. **80**, 4991 (1998).
[6] E. DEKEL, D. GERSHONI, E EHRENFREUND, D. SPEKTOR, J.M. GARCIA, and P.M. PETROFF, Phys. Rev. B **61**, 11009 (2000).
[7] A. BARENCO and M.A. DUPERTUIS, Phys. Rev. B **52**, 2766 (1995).
[8] I. SHTRICHMAN, D. GERSHONI, and R. KALISH, Phys. Rev. B **56**, 1509 (1997).
[9] U. BOCKELMANN, W. HELLER, A. FILORAMO, and PH. ROUSSIGNOL, Phys. Rev. B **55**, 4456 (1997).
[10] G. BACHER, R. WEIGAND, V.D. KULAKOVSKII, N.A. GIPPIUS, A. FORCHEL, K. LEONARDI, and D. HOMMEL, Phys. Rev. Lett. **83**, 4417 (1999).
[11] V. ZWILLER, M.E. PISTOL, D. HESSMAN, R. CEDERSTROM, W. SEIFER, and L. SAMUELSON, Phys. Rev. B **59**, 5021 (1999).
[12] I.N. STRANSKI and L. KRASTANOW, Akad. Wiss. Lit. Mainz Math.-Naturw. Kl. 11b **146**, 767 (1939).
[13] J.M. GARCIA, T. MANKAD, P.O. HOLTZ, P.J. WELLMAN, and P.M. PETROFF, Appl. Phys. Lett. **72**, 3172 (1998).
[14] L.W. WANG, J. KIM, and A. ZUNGER, Phys. Rev. B **59**, 5678 (1999).
[15] O. STIER, M. GRUNDMANN, and D. BIMBERG, Phys. Rev. B **59**, 5688 (1999).
[16] C. PRYOR, Phys. Rev. B **60**, 2869 (1999).
[17] D.S. CITRIN, Phys. Rev. Lett **69**, 3393 (1992).
[18] H. AKIYAMA, S. KOSHIBA, T. SOMEYA, K. WADA, H. NOGE, Y. NAKAMURA, T. INOSHITA, A. SHIMIZU, and H. SAKAKI, Phys. Rev. Lett. **72**, 924 (1994).
[19] D. GERSHONI, M. KATZ, W. WEGSCHEIDER, L. N. PFEIFFER, R. A. LOGAN, and K. WEST, Phys. Rev. B **50**, 8932 (1994).
[20] L.C. ANDREANI, Solid State Commun. **77**, 641 (1991).
[21] B. DEVEAUD, F. CLEROT, N. ROY, K. SATZKE, B. SERMAGE, and D.S. KATZER, Phys. Rev. Lett. **67**, 2355 (1991).